JNS

CLINICAL ARTICLE

J Neurosurg 139:334–343, 2023

Optimizing maximum resection of glioblastoma: Raman spectroscopy versus 5-aminolevulinic acid

Johannes Herta, MD, PhD,[1] Anna Cho, MD,[1] Thomas Roetzer-Pejrimovsky, MD,[2] Romana Höftberger, MD,[2] Wolfgang Marik, MD,[3] Gernot Kronreif, PhD,[4] Tanja Peilnsteiner, BSc,[1] Karl Rössler, MD,[1] and Stefan Wolfsberger, MD[1]

[1]Department of Neurosurgery, Medical University of Vienna; [2]Department of Neurology, Division of Neuropathology and Neurochemistry, Medical University of Vienna; [3]Division of Neuroradiology and Musculoskeletal Radiology, Medical University of Vienna; and [4]Austrian Center for Medical Innovation and Technology (ACMIT), Wiener Neustadt, Austria

OBJECTIVE The objective of this study was to assess and compare the potential of 5-aminolevulinic acid (5-ALA) and Raman spectroscopy (RS) in detecting tumor-infiltrated brain in patients with glioblastoma (GBM).

METHODS Between July 2020 and October 2021, the authors conducted a prospective clinical trial with 15 patients who underwent neurosurgical treatment of newly diagnosed and histologically verified GBM. A solid contrast-enhancing tumor core and peritumoral tissue were investigated intraoperatively for cancer cells by using 5-ALA and RS to achieve pathology-tailored maximum resection. In each case, a minimum of 10 biopsies were sampled from navigation-guided areas. Two neuropathologists examined the biopsies for the presence of neoplastic cells. The detection performance of 5-ALA and RS alone and in combination was assessed. Pre- and postoperative MRI, Karnofsky Performance Status (KPS), and National Institutes of Health Stroke Scale (NIHSS) scores were compared, and median progression-free survival (PFS) was evaluated.

RESULTS A total of 185 biopsy samples were harvested from the contrast-enhancing tumor core (n = 19) and peritumoral tissue (n = 166). In the tumor core, 5-ALA and RS each showed a sensitivity of 100%. In the peritumoral tissue, 5-ALA was less sensitive than RS in detecting cancer (46% vs 69%) but showed higher specificity (81% vs 57%). When the two methods were combined, the accuracy of tumor detection was increased by about 10%.

Pathology-tailored resection led to a 52% increase in resection volume comparing the volume of preoperative contrast enhancement with the postoperative resection cavity on MRI (p = 0.0123). Eloquent brain involvement prevented gross-total resection in 4 patients. Four weeks after surgery, mean KPS (p = 0.7637) and NIHSS scores (p = 0.3146) were not significantly different from preoperative values. Of the 13 patients who had received postoperative chemoradiotherapy, 4 did not show any progression after a median follow-up of 14 months. The remaining 9 patients had a median PFS of 8 months.

CONCLUSIONS According to the study data, RS is capable of detecting tumor-infiltrated brain with higher sensitivity but lower specificity than the current standard of 5-ALA. With further technological and workflow advancements, RS in combination with protoporphyrin IX fluorescence may contribute to pathology-tailored glioma resection in the future.

Clinical trial registration no.: 12597564 (abstimmungen.basg.gv.at)

https://thejns.org/doi/abs/10.3171/2022.11.JNS22693

KEYWORDS Raman spectroscopy; 5-aminolevulinic acid; high-grade glioma; glioblastoma surgery; infiltration zone; oncology; tumor

At 14.6 months, the median survival of glioblastoma (GBM) patients is very poor even with maximum safe resection and adjuvant chemoradiotherapy. The extent of resection plays a decisive prognostic role in progression-free survival (PFS) and probably overall survival.[1]

While the negative impact of MRI T1 contrast-enhancing residual tumor on survival has been confirmed, the role of peritumoral tissue without contrast enhancement has not yet been fully clarified: radiologically, MRI T2 hyperintensity in the peritumoral zone is not specific, reflecting partly vasogenic edema or tumor infiltration.[2] Histo-

ABBREVIATIONS 5-ALA = 5-aminolevulinic acid; CCD = charge-coupled device; CER = contrast-enhanced region; GBM = glioblastoma; GTR = gross-total resection; KPS = Karnofsky Performance Status; NIHSS = National Institutes of Health Stroke Scale; NPV = negative predictive value; NTR = near-total resection; PFS = progression-free survival; PpIX = protoporphyrin IX; PPV = positive predictive value; RS = Raman spectroscopy; STR = subtotal resection; WHO = World Health Organization.

SUBMITTED March 22, 2022. **ACCEPTED** November 16, 2022.

INCLUDE WHEN CITING Published online December 23, 2022; DOI: 10.3171/2022.11.JNS22693.

logically, it is known that peritumoral tissue is biologically heterogeneous and can contain cancer cells.[2,3] These cells have been shown to proliferate more aggressively than the initiating cancer; hence, the peritumoral area is the most common site of tumor recurrence.[4]

To counteract this, the concept of supramaximal resection—that is, the removal of noneloquent peritumoral tissue up to prevailing anatomical limits—has been promulgated.[5] While the results indicate a positive impact on overall survival, there is no consensus on the definition of supramaximal resection limits.[6] This becomes important, as cancer cells, like neural cells, use the same extracellular pathways as blood vessels and white matter tracts to invade the brain.[7] During the subgyral white matter resection outside the contrast-enhancing tumor, surgeons are guided by haptic feedback and neuronavigation, as they are blinded to the presence of tumor infiltration.

To achieve a highly selective and pathology-tailored resection that exceeds the contrast-enhancing tumor, different methods of visualization have been employed. Of all the tissue fluorophores, 5-aminolevulinic acid (5-ALA) has emerged as a standard tool for visualizing the tumor core by strong fluorescence and the surrounding infiltration zone by vague fluorescence from protoporphyrin IX (PpIX) accumulation in malignant glioma cells. The fluorochrome can be visualized intraoperatively by violet-blue light and is used for the identification of residual tumor.[8–12] However, 5-ALA fluorescence assessment is semiquantitative, not pathology-specific, and its negative predictive value (NPV) varies widely between studies (range 22%–91%).[9,12–19]

Other methods of intraoperative tissue interrogation, like confocal laser endomicroscopy or optical coherence tomography, offer resolution on the cellular level in real time. But as they require a trained user to interpret their results, these methods have not yet found their way into routine clinical practice.[20,21] A technology only recently brought into the neurosurgical theater is Raman spectroscopy (RS). It allows real-time discriminatory feedback of tumor tissue on a molecular level and is entity specific. Different types of spectroscopic systems have been introduced that allow assessment of tissue 1) prior to its resection with a single-point RS probe or an endoscopic imager, or 2) after its resection with an already commercially available Raman microscope.[22,23]

In this prospective clinical trial, we used a single-point RS probe as well as 5-ALA fluorescence to guide the resection of GBMs in the infiltration zone. Our aim was to compare their potential in detecting cancer-infiltrated brain and assess the workflow of both methods in 15 patients with GBM.

Methods

Patient Cohort and Study Design

The study was conducted between July 2020 and October 2021 at the Department of Neurosurgery, Medical University of Vienna. Patients between the ages of 18 and 80 years with a GBM newly diagnosed by neuroimaging were eligible for study inclusion if open surgery was the selected treatment option. Exclusion criteria were as follows: 1) tumor involving the cerebellum and/or brainstem, 2) recurrent GBM, 3) medical reasons precluding MRI, 4) Karnofsky Performance Status (KPS) ≤ 60, 5) hypersensitivity to porphyrins and porphyria, 6) renal or hepatic insufficiency, 7) history of invasive malignant tumor within the preceding 5 years, 8) pregnancy/lactation, and 9) pathology inconsistent with GBM after histological examination.

For neurological assessment, we used the National Institutes of Health Stroke Scale (NIHSS) score and KPS at admission and 1 day and 4 weeks after surgery. Median PFS was evaluated.

As standard care, patients underwent radiological assessment via a standardized MRI tumor protocol preoperatively and 48 hours postoperatively (Supplemental Table 1). Pre- and postoperative images were compared to assess 1) residual gadolinium contrast enhancement and 2) the amount of resected tissue volume. Residual enhancement was classified as gross-total resection (GTR) < 0.175 cm^3 (no residual tumor), near-total resection (NTR) 0.175–1 cm^3 (residual tumor possible), and subtotal resection (STR) > 1 cm^3 (residual tumor).

5-Aminolevulinic Acid

All patients received an oral solution of 5-ALA (20 mg/kg body weight, Biosynth AG) approximately 3 hours before the induction of anesthesia. To prevent potential skin phototoxicity after the intake of 5-ALA, all patients were protected from light sources for at least 24 hours. Intraoperative PpIX fluorescence was observed under violet-blue light, which was integrated into the neurosurgical microscopes (Kinevo 900, Carl Zeiss Surgical GmbH). Fluorescence was classified as strong (strong red), vague (less vivid pink), or none.

Raman Spectroscopic Probe

To perform in vivo RS, we used the Sentry S1000 (ODS Medical Inc.), a custom-built handheld probe that consists of a fiber-optic cable connected to a near-infrared spectrum–stabilized laser emitting at 785 nm, which has already been described elsewhere.[24] For Raman detection, the probe is further connected to a high-speed and high-resolution charge-coupled device (CCD) spectroscopic detector. The spectra cover a range of spectral shifts from 381 to 1653 cm^{-1}. The spectral resolution varies between 1.6 and 2.1 cm^{-1} across the spectral domain. Both the laser and the imaging spectrometer are connected to a personal computer for data processing. A custom-built user interface provides control functions, visualizes the Raman spectra in real time, and divides the results of tissue interrogation into cancer or normal tissue (Supplemental Fig. 1).

At the start of every procedure, the CCD was cooled down to −40°C, the sterilized spectroscopic probe was plugged into the laser, and the system carried out a self-test to check for damaged fibers. Before each measurement, the probe tip was cleaned, and the surgeon had to ensure an almost blood-free environment. Measurements, which had a duration of 0.2 seconds, were taken with the lights of the microscope and those of the operating room

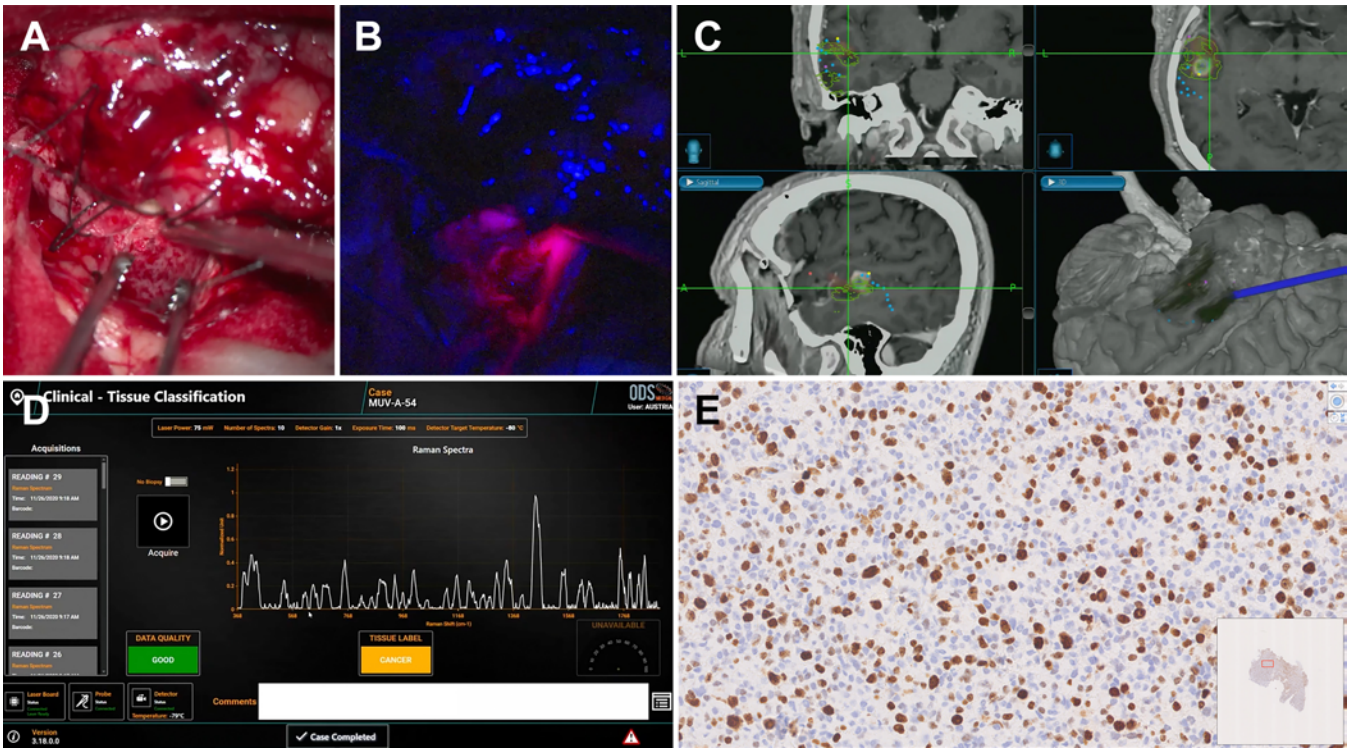

FIG. 1. Investigation of the tumor core. Sampling of central tumor tissue under the surgical microscope (**A**). The tumor shows strong fluorescence of PpIX under blue light (**B**). The location of the sample is taken from MRI contrast-enhancing tumor and marked in the neuronavigation (**C**). Spectra measured by the Raman probe that is classified as cancer by the algorithm (**D**). Results from the Raman measurement as well as strong fluorescence of PpIX are validated by postoperative histopathological examination, which shows a highly proliferative compact GBM, as illustrated by MIB1 staining (**E**, original magnification ×20).

temporarily switched off. During these measurements, the Raman spectroscopic probe had to be in direct but gentle contact with the brain tissue. The sampling depth of the probe has been demonstrated approximately 1 mm beneath the surface.[25]

Data Acquisition During Surgery

Video 1 illustrates the intraoperative workflow of the 5-ALA investigation, RS measurements, and tissue sampling.

VIDEO 1. Workflow of 5-ALA investigation, RS measurements, and tissue sample collection during surgery. © Johannes Herta, published with permission. Click here to view.

Prior to surgery, the surgeon defined regions of eloquent brain that had to be spared during the resection. In all patients, electromagnetic neuronavigation (StealthStation S8, Medtronic) was used for guidance. During every surgery, at least 10 RS measurements and consecutive 5-ALA assessments were performed, and the location was marked on the navigation system. Immediately afterward, a tissue biopsy sample was collected at the exact same position and preserved in formalin for further histological analysis. The distance between the location of the biopsy and the contrast-enhanced region (CER) was measured on MRI and classified as 1) CER, 2) < 10 mm from the CER, and 3) > 10 mm from the CER.

First, the surgeon resected the MRI-defined contrast-enhancing tumor core, which always showed strong 5-ALA positivity. During this step, at least one sample per patient was measured and collected (Fig. 1). Thereafter, the surgeon screened the peritumoral tissue, and at least three measurements and samples were taken from each of the following locations: 1) infiltration zone vaguely positive for 5-ALA (Fig. 2), 2) infiltration zone negative for 5-ALA but positive for RS (Fig. 3), and 3) infiltration zone negative for both 5-ALA and RS (Fig. 4).

If no zone was positive for 5-ALA or RS in peritumoral tissue, the surgeon took three additional measurements and samples. If appropriate for the resection, the surgeon could increase the number of samples taken from each patient.

Neuropathological Processing

All neuropathological analyses were independently performed by two neuropathologists specialized in neurooncology and blinded to any intraoperative information about the acquired measurements. In cases of disagreement between the two reviewers, consensus was established. All tumors were diagnosed according to the 5th edition of the World Health Organization (WHO) Classification of Tumors of the Central Nervous System.[26]

Neoplastic cells were identified on H&E- and MIB1-stained sections based on their morphological features, including nuclear atypia and nuclear polymorphism. The total cancer cell density was estimated for each sample. For further statistical analysis, each sample was classified as

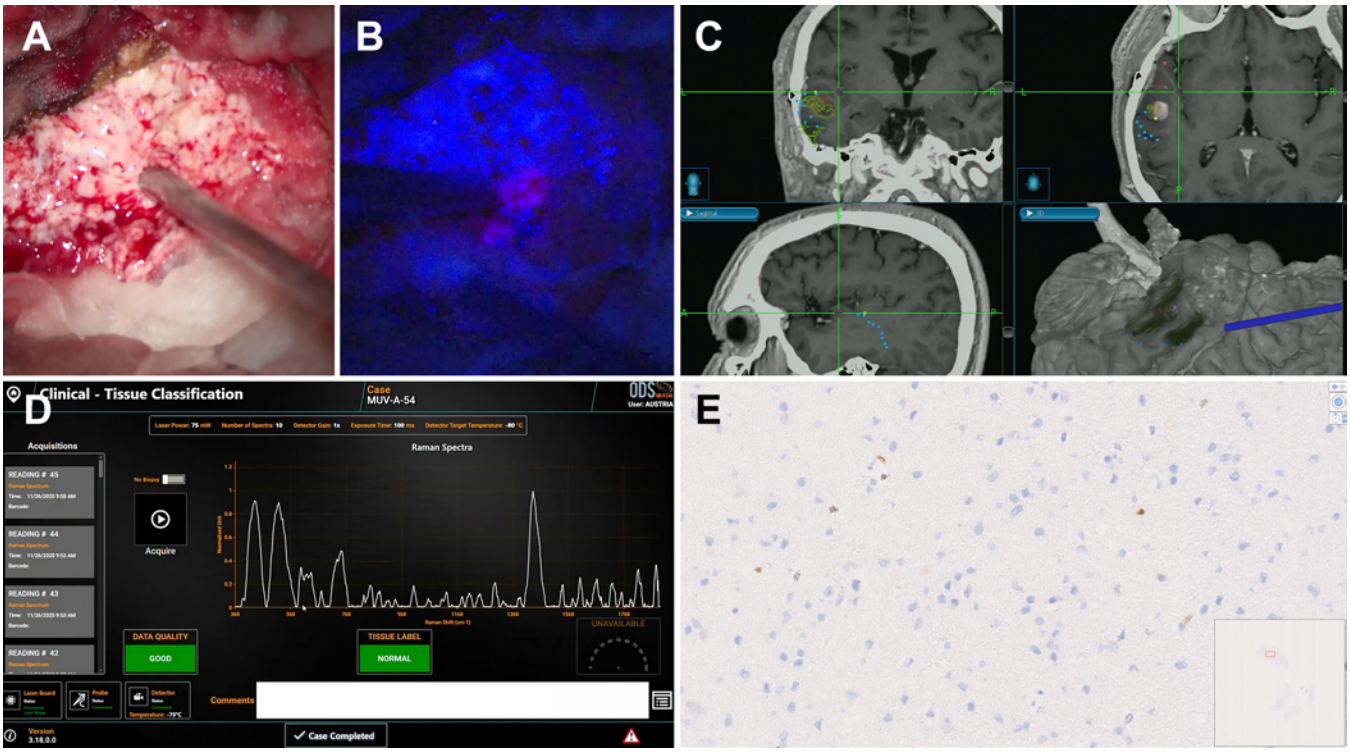

FIG. 2. Investigation of adjacent white matter. During white matter dissection (**A**), a vague fluorescence of PpIX (**B**) indicates the presence of cancer cells. MRI does not show contrast-enhancing tumor at this site (**C**), and the Raman measurement detects normal brain (**D**). The false-positive detection by 5-ALA is validated by the absence of cancer cells in the histopathological analysis (**E**, original magnification ×20).

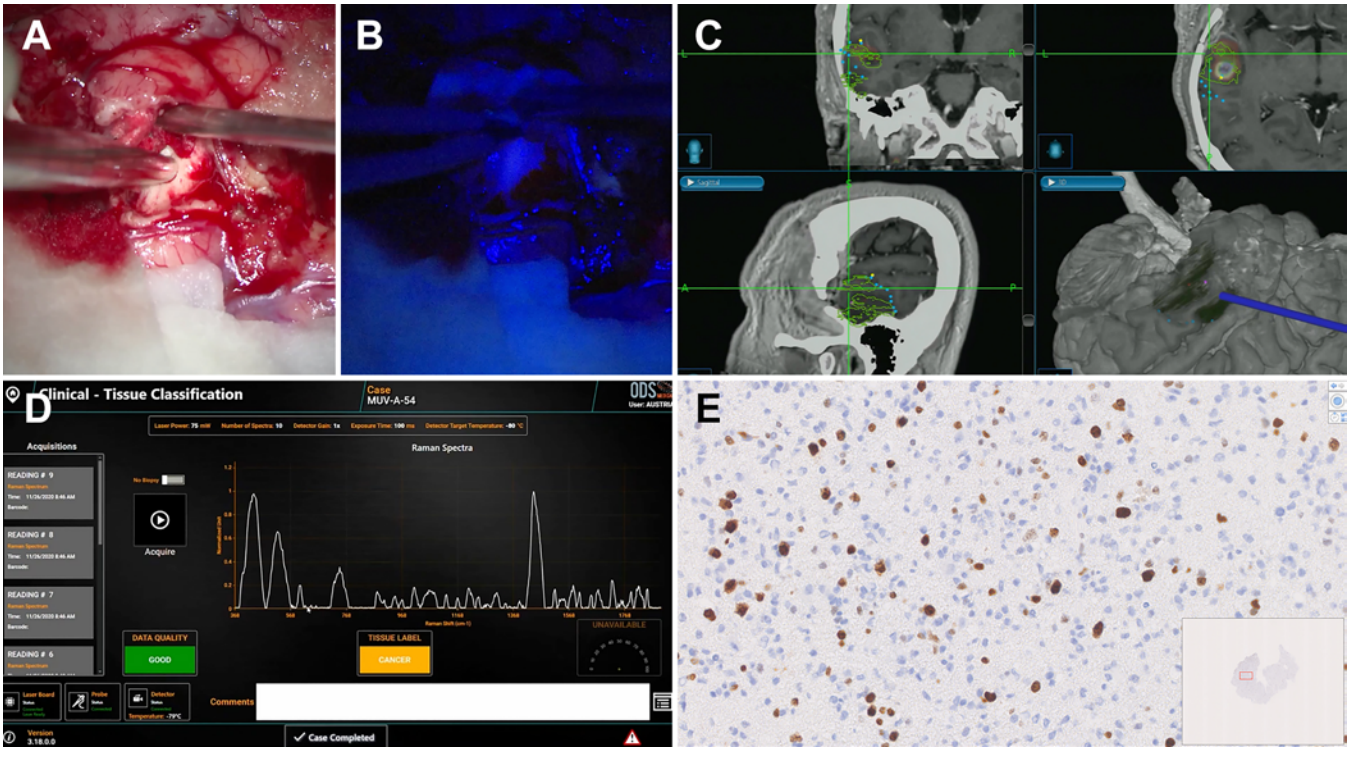

FIG. 3. Investigation of adjacent cortex. A Raman measurement is taken from peritumoral tissue (**A**) and indicates the presence of cancer cells (**D**). But at the sampling location, preoperative MRI does not show contrast-enhancing tumor (**C**), and there is no fluorescence of PpIX (**B**). Nevertheless, MIB1 staining verifies the presence of cancer cells (**E**, original magnification ×20).

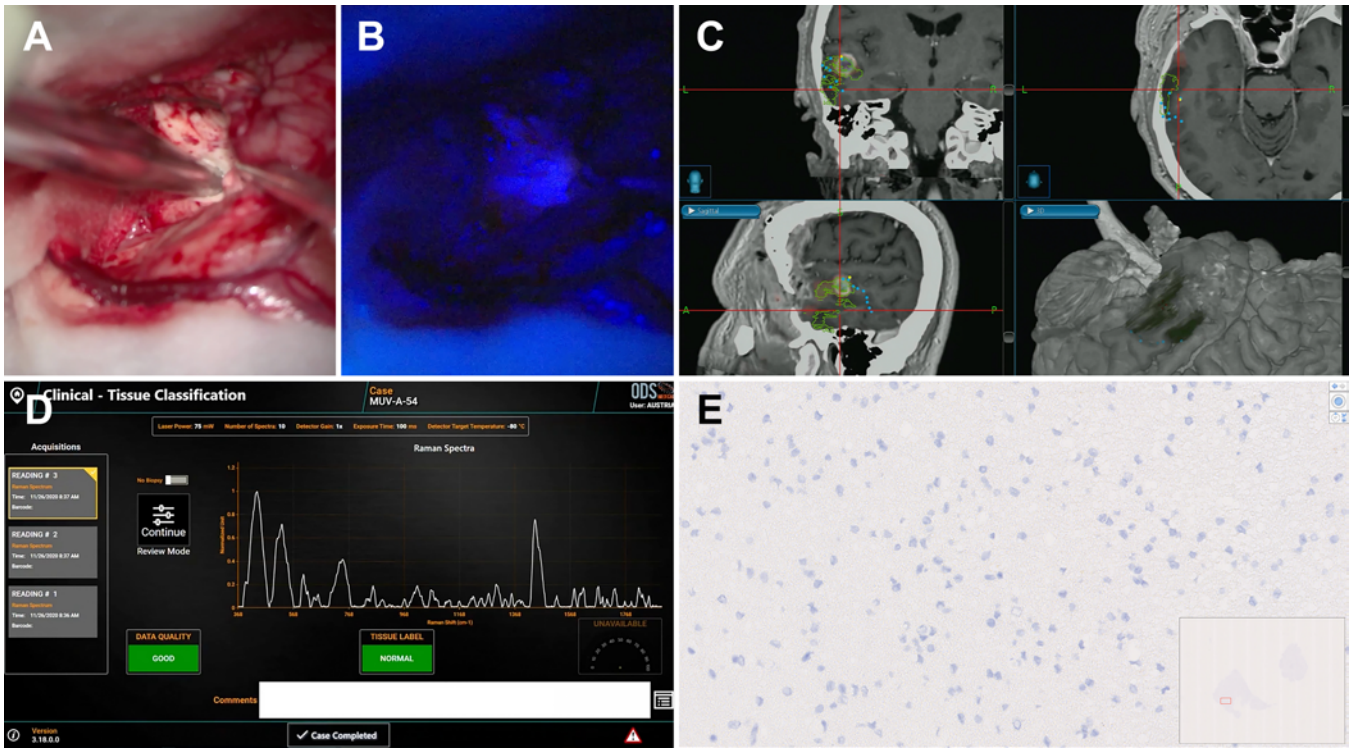

FIG. 4. Investigation of normal brain. After resecting tumor in the middle and superior temporal gyri, the inferior temporal gyrus (**C**) is examined with RS (**A**) and under blue light to detect fluorescence of PpIX (**B**). Both methods indicate normal brain (**D**), and the resection is stopped. Correct measurements are proven by postoperative histopathological analysis, as illustrated by MIB1 staining (**E**, original magnification ×20).

tumor positive if the focal cancer cell density was ≥ 15% or as tumor negative if not. Furthermore, cell counting (total cell count per area) was done based on H&E-stained images. The MIB1 proliferation index was determined for each sample.

For every sample, the presence of necrosis and inflammation was estimated and categorized as 0%, 1%–25%, 26%–50%, or 51%–100%. Blood vessel status was assigned to one of the three categories of inconspicuous, activated, or proliferative. Categories of tissue homogeneity of sampled tissue were implemented, ranging from very inhomogeneous (areas with ≥ 15% cancer cells as well as < 15% cancer cells) to inhomogeneous (cancer cell count in all areas either ≥ 15% or < 15%, but with significant deviations) to homogeneous (nearly no deviations).

Statistical Analysis

For statistical analysis, GraphPad Prism version 9.3.0 was used. A statistical significance level of 0.05 was assumed. Tumor detection performance was calculated by comparing 5-ALA and RS findings with the histopathological results. The ability to detect tumor tissue was compared using the McNemar test adjusted for clustered data according to Durkalski et al.[27] Classification accuracy, sensitivity, specificity, positive predictive value (PPV), and NPV were determined. The confidence intervals for sensitivity and specificity were adjusted for multiple observations by a ratio estimator, as described by Genders et al.[28]

Factors that may influence the tumor detection capabilities of both methods as well as patient characteristics were evaluated by univariate analysis using the Mann-Whitney U-test for nonparametric data and the Student t-test for normally distributed data.

Ethical Approval

The study protocol was approved by the local ethics committee of the Medical University of Vienna and is in accordance with the Helsinki declaration of human rights. Informed consent was obtained from each patient. The Austrian Federal Office for Safety in Health Care approved the use of Sentry S1000 to conduct this clinical investigation, the study is registered with the Austrian Federal Office for Safety in Health Care (abstimmungen.basg.gv.at), and its registration no. is 12597564.

Results

Patient Demographics

Fifteen GBM patients were included in the study (Table 1). The median age was 63 years (range 40–79 years). The predominant localization of the tumor was temporal (n = 8), frontal (n = 3), parietal (n = 3), and occipital (n = 1). The predominant symptoms were seizures (n = 8), confusion (n = 3), aphasia (n = 2), homonymous hemianopia (n = 1), and headache (n = 1). At admission, patients had a mean KPS of 89.3 ± 9.6 and mean NIHSS score of 0.8 ± 1.1.

TABLE 1. Summary of characteristics in 15 GBM patients

Characteristic	Value	p Value
Age in yrs	63 (40–79)	
Female	5 (33)	
Predominant tumor location		
Frontal	3 (20)	
Temporal	8 (53)	
Parietal	3 (20)	
Occipital	1 (7)	
Molecular profile		
IDH-1/2 wild type	14 (93)	
MGMT promoter methylation	5 (33)	
Preop tumor vol in cm^3	26.8 ± 19.7	0.0123
Postop resection vol in cm^3	40.6 ± 28.3	
Residual tumor		
GTR	11 (73)	
NTR	1 (7)	
STR	3 (20)	
Preop NIHSS score	0.8 ± 1.1	0.3146
4-wk postop NIHSS score	0.4 ± 0.6	
Preop KPS	89.3 ± 9.6	0.7637
4-wk postop KPS	88 ± 18.2	
FU in mos, n = 15	13.2 (3–19.5)	
No RTX/CTX	2	
Dead	8	
2nd surgery	4	
No progression at FU	4	
FU in mos	14.4 (11.6–14.6)	
PFS in mos, n = 9	8 (0.8–12.4)	

FU = follow-up; RTX/CTX = combined chemoradiotherapy treatment.
Values are expressed as median (range), number (%), or mean ± standard deviation.

Results of Surgery

GTR was achieved in 11 patients (73%), NTR in 1 (7%), and STR in 3 (20%). In all 4 cases of incomplete resection, the surgeon decided against complete tumor removal because of eloquent involvement. Because our approach of a pathology-tailored resection exceeds the limits of contrast enhancement on MRI, a significant difference of 52% ($p = 0.0123$) could be seen in comparing the mean preoperative tumor volume (26.8 ± 19.7 cm^3) with the mean resected volume (40.6 ± 28.3 cm^3).

Four weeks after surgery, the mean KPS (88 ± 18.2) and NIHSS score (0.4 ± 0.6) were not significantly different from preoperative values (KPS: $p = 0.7637$; NIHSS score: $p = 0.3146$). Neurological deterioration after surgery occurred in only 1 patient who had sensory aphasia as well as impaired cognition after the removal of a left temporal GBM. Three of 15 patients had hydrocephalus 18, 114, and 238 days after surgery and needed cerebrospinal fluid diversion. Other perioperative complications included 1 case with a postoperative intracerebral abscess that required drainage and antibiotic treatment, 1 case with chronic obstructive pulmonary disease who developed pneumonia after being discharged from the hospital, and 1 case that continued to have seizures postoperatively.

After surgery, all but 2 patients underwent combined chemoradiotherapy. One patient refused further treatment after surgery, and another developed fulminant pneumonia that prohibited further treatment. The remaining 13 patients had a median follow-up of 14 months (range 7.5–19.5 months). During the follow-up period, 9/13 patients showed tumor progression with a median PFS of 8 months (range 0.8–12.4 months) and 6/13 patients died with a median survival of 13.6 months (range 9.4–19.5 months). In 8/9 patients with GTR, tumor progression occurred at the former resection limit, while in only 1 case progression was distant. Four of the 9 patients with progression underwent a second surgery. Patients without tumor progression during the study period (4/13) had a median follow-up of 14.4 months.

Tumor Detection Properties of 5-ALA and RS

A total of 185 biopsy samples were taken from 15 patients. The distribution of the samples as well as the recorded 5-ALA and RS status is listed in Table 2. Altogether, 19 samples were taken from the tumor core strongly positive for 5-ALA, whereas 166 samples were taken from peritumoral tissue.

Tumor Core

All 19 samples taken from the histologically verified and contrast-enhancing tumor core showed strong fluorescence of PpIX intraoperatively. The same was found for RS measurements, which indicated cancer in all 19 measurements (Fig. 1).

Peritumoral Tissue

In 166 peritumoral tissue samples, a focal cancer cell density of ≥ 15% was found in 111 samples. Table 3 shows an overview of the tumor detection capabilities of RS and 5-ALA. The accuracy in detecting cancer cells with RS was 63% compared to 61% with 5-ALA. While RS showed a higher sensitivity at 69% versus 46%, 5-ALA showed

TABLE 2. Number and location of biopsy samples taken in 15 patients with GBM

Zone	5-ALA+ & RS+	5-ALA– & RS–	5-ALA+ & RS–	5-ALA– & RS+	Total
Tumor core	19	0	0	0	19
Peritumoral tissue	40	55	16	55	166
CER	15	12	4	10	41
<10 mm from CER	21	23	6	31	81
>10 mm from CER	4	20	6	14	44

TABLE 3. Tumor detection properties of 5-ALA and RS in the infiltration zone, estimated focal tumor cell count ≥ 15%

Modality	Accuracy (95% CI)	Sensitivity (95% CI)	Specificity (95% CI)	PPV (95% CI)	NPV (95% CI)
5-ALA	0.61 (0.54–0.69)	0.46 (0.36–0.56), (0.38–0.54)*	0.81 (0.72–0.90), (0.70–0.92)*	0.75 (0.66–0.84)	0.55 (0.45–0.64)
RS	0.63 (0.56–0.71)	0.69 (0.59–0.78), (0.59–0.78)*	0.57 (0.46–0.68), (0.42–0.72)*	0.66 (0.57–0.76)	0.59 (0.48–0.71)
5-ALA & RS combined†	0.73 (0.64–0.82)	0.61 (0.49–0.74), (0.51–0.72)*	0.89 (0.80–0.99), (0.75–1)*	0.90 (0.82–0.98)	0.61 (0.48–0.74)

* Confidence interval adjusted for multiple observations by a ratio estimator.
† Without inconclusive measurements.

higher specificity at 81% versus 57% for RS. Both methods alone showed a similar NPV: 55% for 5-ALA and 59% for RS. An adjusted McNemar test showed that diagnosing cancer cells in the infiltration zone with RS is statistically significantly more sensitive than with 5-ALA ($p = 0.018$).

If both methods show concordant results, a combined detection performance with a sensitivity of 61% and specificity of 89% is shown and accuracy is increased about 10%.

Univariate analysis of potential factors that influence the detection performance of RS in peritumoral tissue showed that the detection of cancer cells depended on vascularization ($p = 0.0129$), MIB1 proliferation index ($p = 0.0038$), and cellularity ($p = 0.0039$). The presence of inflammation ($p = 0.1259$) or necrosis ($p = 0.1591$), tissue homogeneity ($p = 0.7573$), and distance from the biopsy site to the CER ($p = 0.2019$) did not show any influence. Interestingly, for 5-ALA, none of the previously mentioned factors had an influence: vascularization ($p = 0.5696$), MIB1 proliferation index ($p = 0.1166$), cellularity ($p = 0.1537$), presence of inflammation ($p = 0.6133$) or necrosis ($p = 0.6493$), tissue homogeneity ($p = 0.0631$), and distance from the biopsy site to the CER ($p = 0.8569$).

A detailed list of the pros and cons of both methods in detecting GBM cancer cells in peritumoral tissue appears in Table 4.

Discussion

The intraoperative detection of GBM cells is profoundly important, as residual cancer cells negatively impact tumor recurrence and survival time.[1] Since neuronavigation is limited by brain shift and MRI contrast enhancement of the tumor relies on disruption of the blood-brain barrier, several techniques have been proposed to intraoperatively visualize the tumor and guide surgery independent from neuronavigation.[11,29] The present work is the first to compare the in vivo detection performance of two major guiding techniques: RS and 5-ALA.

Raman Spectroscopy

While 5-ALA has emerged as a standard neurosurgical tool to visualize cancer cells intraoperatively,[8–12] the in vivo use of RS is still in its infancy.[25,30–32] The reason for this is the difficulty in reliably and safely examining biological tissue, as it produces a low Raman signal that stands out only slightly from its background and is heavily contaminated by autofluorescence signals from tissue and instruments.[22]

The first human in vivo application of RS was described by Jermyn et al. in 2015.[25] These authors used a system (Emvision LLC) with a handheld optical probe that discriminated brain tissue from tumor tissue in 17 glioma patients with an accuracy of 90% and a sensitivity and specificity of 93% and 91%, respectively. Of the 161 samples that were evaluated, 68 (42%) were taken from WHO grade IV gliomas. Even in looking at only the 56 samples that histologically showed tumor invasion, similarly good results were shown with an accuracy of 90%, a sensitivity of 89%, and a specificity of 91%. After further improvements to the Raman system, the same research group was able to confirm its good results for glioma and brain metastasis patients.[30]

In our study we used an updated version of the described Raman system (Sentry S1000), which displays its results as the dichotomous tissue labels of "cancer" or "normal" brain. Each of the 19 samples taken from the MRI con-

TABLE 4. Pros and cons of using 5-ALA and RS to detect tumor cells in the infiltration zone of GBMs

Parameter	RS	5-ALA
Detection performance	Higher sensitivity, lower specificity	Lower sensitivity, higher specificity
Measurements affected by	Ambient light (microscope & infrared light of neuronavigation need to be switched off during measurements), tissue covered by blood, used classifier	Ambient light (insufficient illumination of nonfluorescing areas), tissue covered by blood, time of 5-ALA intake, mode of observation (ocular vs monitor), photobleaching
Availability	No exogenous compound used, immediately available, probe sterilization required	Intake latency must be considered, no acute surgery possible, patients should not be exposed to light if surgery postponed for 24–48 hrs
Measurement properties	Focal measurement w/ delay in range of seconds, entity specific (classifier), binary output from quantitative measurement	Global surface measurement with real-time guidance, not specific for GBM, qualitative measurement
Application in GBM recurrence, postradiation	No data available yet	Lower specificity & NPV in CERs,[41] no data available for infiltration zone

trast-enhancing tumor core were also correctly detected as tumor by the probe. However, looking at the 166 samples taken from peritumoral tissue, we found results contradictory to those previously published, with a detection accuracy of 63%, sensitivity of 69%, and specificity of only 57%. However, it must be noted that in the study by Jermyn et al., it remains unclear how many biopsies in GBM patients originated from the tumor core or from the peritumoral tissue. In addition, they chose a different pathohistological cutoff in their study, that is, the presence of ≤ 90% cancer cells to classify as infiltrated brain.[25]

Because RS is very susceptible to interference, care was taken to ensure that optimal conditions prevailed for each measurement. The probe was tested for fiber integrity before each use and cleaned with a fine cotton cloth before each measurement. Bloodless conditions were created before each measurement. The ambient light was switched off except for the necessary monitors, and electromagnetic navigation instead of optical infrared navigation was used.

In contrast to authors of previous studies, we used an existing classifier and could not compare the individual Raman spectra to investigate differences in the molecular signature of the samples. Nevertheless, we were able to show with our measurements that a correct determination by RS depended on an increased MIB1 proliferation index ($p = 0.0038$), high cellularity ($p = 0.0039$), and the increased presence of vascularization ($p = 0.0129$).

5-Aminolevulinic Acid

Histopathological studies comparing PpIX fluorescence and histopathological findings in peritumoral tissue of GBM are rare, and definitions of the solid tumor core and the infiltration zone are heterogeneously used in the literature. In our study, we used a surgically oriented definition. The central tumor core was neuroradiologically limited by the contrast-enhancing tumor rim present on preoperative MRI but also visible because of its strong PpIX fluorescence, which was removed as the first step of every operation. The infiltration zone in the peritumoral tissue was then histopathologically defined by the presence of ≥ 15% of focal cancer cells.

With these definitions, we observed that 5-ALA showed strong positive fluorescence in all 19 tumor core biopsies with a sensitivity of 100%, which is consistent with the high values of around 90% in the literature.[9,12–14,16–18] Strong fluorescence is known to be associated with higher cell density, solidly proliferating tumor, and increased fluorescence in spectroscopy.[19]

In the 166 peritumoral tissue biopsies, however, PpIX fluorescence showed an accuracy of 61%, a sensitivity of only 46%, and a specificity of 81% in detecting tumor in the infiltration zone, which was independent from vascularization ($p = 0.5696$), MIB1 proliferation index ($p = 0.1166$), cellularity ($p = 0.1537$), and the presence of inflammation ($p = 0.6133$) or necrosis ($p = 0.6493$). Better results were found in five prospective trials that investigated the detection performance of 5-ALA after maximal white light resection.[13,17,18,33,34] Detection sensitivities from around 90% and specificities around 53% to 89% were found in newly diagnosed as well as recurrent GBM.[13,17,18] Even the investigation of exclusively recurrent GBM revealed a PPV of 97% for 5-ALA in detecting tumor, compared to 75% in our study.[34] Stummer et al. observed a PPV of 92% after solid tumor debulking if vague florescence was present in 33 patients with newly diagnosed GBM.[33] Nevertheless, false-positive fluorescing biopsies in the vicinity of the tumor have been described in the literature.[16,33–35] So far, the cause has been considered to be linked with reactive astrocytes, autofluorescence of normal brain, or radiation necrosis.[13,14,36] Of 14/166 false-positive biopsies from 7/15 patients, 4 samples showed reactive changes and 2 samples showed a transition into an infarct area.

False-negative results occur far more often and can be attributed to a wide range of causes such as 1) a low number of cancer cells, 2) structural barriers that interfere with fluorescence visualization, 3) the timing of 5-ALA administration, and 4) tumor necrosis.[37] In our study 50 biopsy samples from 14/15 patients showed false-negative results. While the timing of 5-ALA administration was applied according to the protocol and we tried to optimize the visualization of fluorescence, effects like photobleaching cannot be counteracted. In most false-negative biopsies a low number of cancer cells was estimated, while in 9/50 samples dense cancer cells were encountered. In only one of these cases, the error could be explained by necrosis.

Pathology-Tailored Resection

Safe and complete resection of contrast-enhancing tumor is seen as the optimal goal in GBM surgery.[5] However, GTR is seldom achieved, as it highly depends on tumor location, surgeon experience, and technical adjuncts to identify tumor intraoperatively. Moreover, the migratory behavior of GBM cells and their heterogeneity make it difficult to distinguish tumor-infiltrated brain from normal brain, which is one of the main challenges in neurosurgery to date and has led to the technique of "supramaximal" or "supratotal" resection in GBM surgery.[6,38] No unified definition exists for supramaximal resection, but in general it involves resecting beyond the contrast-enhancing margins, which has shown an impact on overall survival in preliminary studies.[5]

With the techniques now available to us, we propose a pathology-tailored resection. As always, it is important to emphasize that the possible resection is limited by the presence of eloquent brain areas and findings on intraoperative neuromonitoring.

On the cortical surface it is possible to use sulcal boundaries as a limit for resection. If the attached gyrus does not show any abnormalities on MRI, it is inspected for the presence of cancer cells by means of blue light but also with a Raman probe. Here, RS shows an advantage over 5-ALA, as the cortical boundary can be maintained, which is often not the case with 5-ALA if it shows only vague fluorescence.

Subsequently, dissection begins in the white matter, which is more challenging given the absence of anatomical boundaries along the fiber tracts. 5-ALA is a convenient method to perform real-time guided tumor resection. If 5-ALA negativity is achieved, the resection limits can be controlled with the more sensitive Raman probe to identify further tumor extensions growing along fiber tracts.[39]

A pathology-tailored resection followed by chemora-

diotherapy was possible in 9 of the 15 patients without the occurrence of postoperative neurological deficits. The median PFS for this specific group was 7.1 months, and 4 patients did not show progression after a median follow-up of 14.4 months. In a meta-analysis including 565 patients treated with 5-ALA–guided GBM resection alone, a mean time to tumor progression of 8.1 months was found and is in accordance with our unfinished results.[40]

Limitations

In contrast to IDH-mutant gliomas, there is no histological staining to specifically identify IDH–wild type glioma cells. Thus, the assessment of cancer cell density remains an estimate. However, the reliability of this estimate is high, as the cancer cell density was independently evaluated by two neuropathologists on H&E and MIB1 stainings and intratumoral heterogeneity was additionally considered.

Future Prospects

To apply RS in routine neurosurgery, technological and workflow advancements are still required: reference databases are already being developed to improve existing classifiers and establish new ones for GBMs as well as different tumor types. For gliomas, a single tumor entity should be determined, and a more detailed diagnosis on a molecular basis is the ultimate goal. Therefore, abundant and standardized ex vivo Raman measurements of biopsy samples that undergo histopathological and molecular biological classification are necessary.

Furthermore, integrating the system into the surgical workflow requires improvement. The influence of the operating room light on the Raman measurements, which currently require darkness, and the lack of integration of the Raman probe with the microscope and the navigation system are challenges that need to be resolved if integration into the clinical routine is the goal.

Conclusions

The ability of RS to obtain an entity-specific analysis within seconds at a molecular level is unique and opens a variety of surgical applications. According to our data, RS detects solid tumors flawlessly and is capable of detecting tumor-infiltrated brain in peritumoral tissue with higher sensitivity but lower specificity than the current standard of 5-ALA. With further technological and workflow advancements, the combination of RS and PpIX fluorescence may contribute to pathology-tailored glioma resection in the future.

Acknowledgments

We thank University Professor Dr. Harald Heinzl and Dr. Matthias Tomschik, who supported us with their biostatistical expertise.

References

1. Delgado-López PD, Corrales-García EM. Survival in glioblastoma: a review on the impact of treatment modalities. *Clin Transl Oncol*. 2016;18(11):1062-1071.
2. Lemée JM, Clavreul A, Aubry M, et al. Characterizing the peritumoral brain zone in glioblastoma: a multidisciplinary analysis. *J Neurooncol*. 2015;122(1):53-61.
3. Lemée JM, Clavreul A, Menei P. Intratumoral heterogeneity in glioblastoma: don't forget the peritumoral brain zone. *Neuro Oncol*. 2015;17(10):1322-1332.
4. Ruiz-Ontañon P, Orgaz JL, Aldaz B, et al. Cellular plasticity confers migratory and invasive advantages to a population of glioblastoma-initiating cells that infiltrate peritumoral tissue. *Stem Cells*. 2013;31(6):1075-1085.
5. Li YM, Suki D, Hess K, Sawaya R. The influence of maximum safe resection of glioblastoma on survival in 1229 patients: can we do better than gross-total resection? *J Neurosurg*. 2016;124(4):977-988.
6. Dimou J, Beland B, Kelly J. Supramaximal resection: a systematic review of its safety, efficacy and feasibility in glioblastoma. *J Clin Neurosci*. 2020;72:328-334.
7. Cuddapah VA, Robel S, Watkins S, Sontheimer H. A neurocentric perspective on glioma invasion. *Nat Rev Neurosci*. 2014;15(7):455-465.
8. Aldave G, Tejada S, Pay E, et al. Prognostic value of residual fluorescent tissue in glioblastoma patients after gross total resection in 5-aminolevulinic acid-guided surgery. *Neurosurgery*. 2013;72(6):915-921.
9. Díez Valle R, Tejada Solis S, Idoate Gastearena MA, García de Eulate R, Domínguez Echávarri P, Aristu Mendiroz J. Surgery guided by 5-aminolevulinic fluorescence in glioblastoma: volumetric analysis of extent of resection in single-center experience. *J Neurooncol*. 2011;102(1):105-113.
10. Schucht P, Beck J, Abu-Isa J, et al. Gross total resection rates in contemporary glioblastoma surgery: results of an institutional protocol combining 5-aminolevulinic acid intraoperative fluorescence imaging and brain mapping. *Neurosurgery*. 2012;71(5):927-936.
11. Roessler K, Becherer A, Donat M, Cejna M, Zachenhofer I. Intraoperative tissue fluorescence using 5-aminolevolinic acid (5-ALA) is more sensitive than contrast MRI or amino acid positron emission tomography (^{18}F-FET PET) in glioblastoma surgery. *Neurol Res*. 2012;34(3):314-317.
12. Stummer W, Novotny A, Stepp H, Goetz C, Bise K, Reulen HJ. Fluorescence-guided resection of glioblastoma multiforme by using 5-aminolevulinic acid-induced porphyrins: a prospective study in 52 consecutive patients. *J Neurosurg*. 2000;93(6):1003-1013.
13. Panciani PP, Fontanella M, Schatlo B, et al. Fluorescence and image guided resection in high grade glioma. *Clin Neurol Neurosurg*. 2012;114(1):37-41.
14. Panciani PP, Fontanella M, Garbossa D, Agnoletti A, Ducati A, Lanotte M. 5-aminolevulinic acid and neuronavigation in high-grade glioma surgery: results of a combined approach. *Neurocirugia (Astur)*. 2012;23(1):23-28.
15. Idoate MA, Díez Valle R, Echeveste J, Tejada S. Pathological characterization of the glioblastoma border as shown during surgery using 5-aminolevulinic acid-induced fluorescence. *Neuropathology*. 2011;31(6):575-582.
16. Roberts DW, Valdés PA, Harris BT, et al. Coregistered fluorescence-enhanced tumor resection of malignant glioma: relationships between δ-aminolevulinic acid-induced protoporphyrin IX fluorescence, magnetic resonance imaging enhancement, and neuropathological parameters. Clinical article. *J Neurosurg*. 2011;114(3):595-603.
17. Coburger J, Engelke J, Scheuerle A, et al. Tumor detection with 5-aminolevulinic acid fluorescence and Gd-DTPA-enhanced intraoperative MRI at the border of contrast-enhancing lesions: a prospective study based on histopathological assessment. *Neurosurg Focus*. 2014;36(2):E3.
18. Yamada S, Muragaki Y, Maruyama T, Komori T, Okada Y. Role of neurochemical navigation with 5-aminolevulinic acid during intraoperative MRI-guided resection of intracranial

malignant gliomas. *Clin Neurol Neurosurg*. 2015;130:134-139.
19. Stummer W, Rodrigues F, Schucht P, et al. Predicting the "usefulness" of 5-ALA-derived tumor fluorescence for fluorescence-guided resections in pediatric brain tumors: a European survey. *Acta Neurochir (Wien)*. 2014;156(12):2315-2324.
20. Charalampaki P, Javed M, Daali S, Heiroth HJ, Igressa A, Weber F. Confocal laser endomicroscopy for real-time histomorphological diagnosis: our clinical experience with 150 brain and spinal tumor cases. *Neurosurgery*. 2015;62(suppl 1):171-176.
21. Fan Y, Xia Y, Zhang X, et al. Optical coherence tomography for precision brain imaging, neurosurgical guidance and minimally invasive theranostics. *Biosci Trends*. 2018;12(1):12-23.
22. DePaoli D, Lemoine É, Ember K, et al. Rise of Raman spectroscopy in neurosurgery: a review. *J Biomed Opt*. 2020;25(5):1-36.
23. Hollon TC, Pandian B, Adapa AR, et al. Near real-time intraoperative brain tumor diagnosis using stimulated Raman histology and deep neural networks. *Nat Med*. 2020;26(1):52-58.
24. Desroches J, Jermyn M, Mok K, et al. Characterization of a Raman spectroscopy probe system for intraoperative brain tissue classification. *Biomed Opt Express*. 2015;6(7):2380-2397.
25. Jermyn M, Mok K, Mercier J, et al. Intraoperative brain cancer detection with Raman spectroscopy in humans. *Sci Transl Med*. 2015;7(274):274ra19.
26. Louis DN, Perry A, Wesseling P, et al. The 2021 WHO Classification of Tumors of the Central Nervous System: a summary. *Neuro Oncol*. 2021;23(8):1231-1251.
27. Durkalski VL, Palesch YY, Lipsitz SR, Rust PF. Analysis of clustered matched-pair data. *Stat Med*. 2003;22(15):2417-2428.
28. Genders TS, Spronk S, Stijnen T, Steyerberg EW, Lesaffre E, Hunink MG. Methods for calculating sensitivity and specificity of clustered data: a tutorial. *Radiology*. 2012;265(3):910-916.
29. Arbizu J, Tejada S, Marti-Climent JM, et al. Quantitative volumetric analysis of gliomas with sequential MRI and ^{11}C-methionine PET assessment: patterns of integration in therapy planning. *Eur J Nucl Med Mol Imaging*. 2012;39(5):771-781.
30. Jermyn M, Mercier J, Aubertin K, et al. Highly accurate detection of cancer *in situ* with intraoperative, label-free, multimodal optical spectroscopy. *Cancer Res*. 2017;77(14):3942-3950.
31. Desroches J, Jermyn M, Pinto M, et al. A new method using Raman spectroscopy for in vivo targeted brain cancer tissue biopsy. *Sci Rep*. 2018;8(1):1792.
32. Desroches J, Lemoine É, Pinto M, et al. Development and first in-human use of a Raman spectroscopy guidance system integrated with a brain biopsy needle. *J Biophotonics*. 2019;12(3):e201800396.
33. Stummer W, Tonn JC, Goetz C, et al. 5-Aminolevulinic acid-derived tumor fluorescence: the diagnostic accuracy of visible fluorescence qualities as corroborated by spectrometry and histology and postoperative imaging. *Neurosurgery*. 2014;74(3):310-320.
34. Nabavi A, Thurm H, Zountsas B, et al. Five-aminolevulinic acid for fluorescence-guided resection of recurrent malignant gliomas: a phase II study. *Neurosurgery*. 2009;65(6):1070-1077.
35. Ando T, Kobayashi E, Liao H, et al. Precise comparison of protoporphyrin IX fluorescence spectra with pathological results for brain tumor tissue identification. *Brain Tumor Pathol*. 2011;28(1):43-51.
36. Kamp MA, Felsberg J, Sadat H, et al. 5-ALA-induced fluorescence behavior of reactive tissue changes following glioblastoma treatment with radiation and chemotherapy. *Acta Neurochir (Wien)*. 2015;157(2):207-214.
37. Hadjipanayis CG, Widhalm G, Stummer W. What is the surgical benefit of utilizing 5-aminolevulinic acid for fluorescence-guided surgery of malignant gliomas? *Neurosurgery*. 2015;77(5):663-673.
38. Khalafallah AM, Rakovec M, Bettegowda C, et al. A crowdsourced consensus on supratotal resection versus gross total resection for anatomically distinct primary glioblastoma. *Neurosurgery*. 2021;89(4):712-719.
39. Esmaeili M, Stensjøen AL, Berntsen EM, Solheim O, Reinertsen I. The direction of tumour growth in glioblastoma patients. *Sci Rep*. 2018;8(1):1199.
40. Eljamel S. 5-ALA fluorescence image guided resection of glioblastoma multiforme: a meta-analysis of the literature. *Int J Mol Sci*. 2015;16(5):10443-10456.
41. Broekx S, Weyns F, De Vleeschouwer S. 5-Aminolevulinic acid for recurrent malignant gliomas: a systematic review. *Clin Neurol Neurosurg*. 2020;195:105913.

Disclosures

Dr. Wolfsberger reports being a consultant for and receiving clinical or research support for the study described from Medtronic.

Author Contributions

Conception and design: Wolfsberger, Herta, Kronreif. Acquisition of data: Wolfsberger, Herta, Cho, Kronreif, Peilnsteiner. Analysis and interpretation of data: Herta, Cho, Roetzer-Pejrimovsky, Höftberger, Marik. Drafting the article: Herta. Critically revising the article: Wolfsberger, Cho, Roetzer-Pejrimovsky, Kronreif. Reviewed submitted version of manuscript: Wolfsberger, Herta, Cho, Roetzer-Pejrimovsky, Höftberger, Marik, Kronreif, Rössler. Approved the final version of the manuscript on behalf of all authors: Wolfsberger. Administrative/technical/material support: Herta, Cho, Kronreif, Peilnsteiner. Study supervision: Wolfsberger, Rössler.

Supplemental Information

Videos

Video 1. https://vimeo.com/772488247.

Online-Only Content

Supplemental material is available with the online version of the article.

Supplemental Table and Figure. https://thejns.org/doi/suppl/10.3171/2022.11.JNS22693.

Correspondence

Stefan Wolfsberger: Medical University of Vienna, Austria. stefan.wolfsberger@meduniwien.ac.at.